P 4.1

Doppler Radar Data Assimilation over Terrain using Ensemble Kalman Filter

Yu-Chieng Liou[1,2] Guo-Jhen Huang[1] Ming Xue[3] and Mingjing Tong[3]

[1]Department of Atmospheric Sciences, National Central University, Jhongli, Taiwan

[2]National Science and Technology Center for Disaster Reduction, Taiwan

[3]Center for Analysis and Prediction of Storms, University of Oklahoma, USA

1. Introduction:

The Ensemble Kalman Filter (EnKF) uses an ensemble of model forecasts to compute the covariances between the observed and unobserved parameters, and convey the observed information throughout the space as well as to other variables. The EnKF system contains at least the following three major advantages: (1) the adjoint of the forecast model is not needed; (2) it is less dependent of the prediction model than the 4DVAR method. Evensen (1994) first suggested the usage of EnKF to conduct data assimilation for a nonlinear quasi-geostrophic ocean model. In radar meteorology, Snyder and Zhang (2003) first applied this method for the cloud scale data assimilation using Doppler radar observed radial winds. Based on a compressible nonhydrostatic model with warm rain processes and ice microphysics, Tong and Xue (2005) developed an EnKF system to study the impact of assimilating the Doppler radial wind and/or reflectivity on the recovery of the complete model state. Xue et al. (2006) investigated the performance of an Ensemble Square Root Kalman Filter (EnSRF; Whitaket and Hamill 2002) in assimilating data collected by radar networks. In this study, we designed a series of OSSE-type numerical tests, and applied the EnSRF over flat surface as well as an idealized north-south elongated mountain similar to the terrain on the western side of the Taiwan island.

Corresponding author address: Dr. Y.-C. Liou, Department of Atmospheric Sciences, National Central University, Taiwan, tyliou@atm.ncu.edu.tw.

Our experimental designs particularly focus on studying the issues of quantitative precipitation forecast (QPF), and the impact of the blockage of the radar beams by the terrain on the model assimilation/forecasts products. Some preliminary results will be presented.

2. The Method of EnSRF.

In an EnSRF system the observations are not perturbed. The update of the state variables from the forecast ensemble averages (denoted by an over bar) $\bar{x}^f$ to analysis mean $\bar{x}^a$, and the perturbation of *i*-th member from $x_i'^f$ to $x_i'^a$, can be expressed by:

$$\bar{x}^a = \bar{x}^f + \boldsymbol{K}[\,y^o - H(\bar{x}^f)] \quad (1)$$

$$x_i'^a = (\boldsymbol{I} - \alpha\,\boldsymbol{KH})\,x_i'^f \quad (2)$$

$$\boldsymbol{K} = \boldsymbol{BH}^T(\boldsymbol{HBH}^T + \boldsymbol{R})^{-1} \quad (3)$$

$$\alpha = \{1 + [\boldsymbol{R}/(\boldsymbol{HBH}^T + \boldsymbol{R})]^{1/2}\}^{-1} \quad (4)$$

where $\boldsymbol{K}$ is the Kalman gain matrix; $\boldsymbol{B}$ and $\boldsymbol{R}$ are the error covariance of forecasts and observations, respectively. The observation operator *H*, and its linearized version $\boldsymbol{H}$, project the state variables to the observations y^o. This projection usually consists of spatial and temporal interpolations, and transformations from model state variables to observed parameters. Furthermore, the estimations of $\boldsymbol{BH}^T$ and $\boldsymbol{HBH}^T$ in (3) can be achieved by:

$$\boldsymbol{BH}^T \cong \frac{1}{N-1}\sum_i^N (x_i^f - \bar{x}^f)[H(x_i^f) - \overline{H(x_i^f)}]^T \quad (5)$$

$$\boldsymbol{HBH}^T \cong \frac{1}{N-1}\sum_i^N [H(x_i^f) - \overline{H(x_i^f)}][H(x_i^f) - \overline{H(x_i^f)}]^T \quad (6)$$

where N is the total number of ensembles. The update described above is performed using observation one at a time, so that the numerator and denominator in (4) inside the square root all become scalars. In addition, the influence of each data point is limited within a certain range. After all observations are analyzed, an ensemble of model forecasts continues until the time when the next observations are available.

3. Experimental Design:

In this study the numerical experiments are conducted using the Advanced Regional Prediction System (ARPS). The model setup contains $35 \times 35 \times 35$ grid points, and the horizontal and vertical resolutions are 2.0 and 0.5 km, respectively. In addition to wind, temperature and pressure, the model contains 6 microphysical parameters, they are: q_v , q_c , q_r , q_i , q_s and q_h. For more details of this model, one can refer to Xue et al. (2000; 2001).

Experiment 1: without terrain

This numerical experiment is performed over a flat surface. The radar-observed radial wind and reflectivity data are assimilated into the model to update all the other model state variables. Two tests are explored. In the first test the assimilation window starts from T=25 min, and ends at T=80 min, with an interval of 5 min, which is a typical scanning time period for operational radar. In the second test the assimilation window is from T=55 to 80 min. Therefore, the assimilations are performed 12 and 6 times in the first and second tests, respectively, but end at the same time (T=80 min). Figure 1 shows the radar reflectivity and wind field at Z=2.5 km at T=80, 100, 120 and 140 min. Note that the assimilation ends at T=80 min, after that the model starts to make forecasts. Figure 2 portrays the accumulated rainfall over every 5 min. Figure 3 illustrates the spatial correlation coefficient with respect to the true solution, and the so-called Gilbert Skill Score (Schaefer, 1990) for these two tests. When computing this score, the "event" is defined as an accurate forecast, at a given grid point, of the accumulated rainfall exceeding 1.0 mm over 5 min. It can be seen that in test 1 the correlation remains higher than that of test 2. If 0.5 is used as a threshold value, then test 1 reveals that after assimilating the radar data for 12 times, reliable QPF information can last until T=160 min, or 80 min after the last data insertion. The right panel of Fig. 3 demonstrates that more assimilation produces better results. If 0.5 (0.3) is used as a threshold value of the Gilbert Skill Score, then the QPF results remain meaningful 60 (90) min after the last assimilation. In this experiment it can be found that if a 60-min of QPF is needed, then at least 12 times of data assimilation is required. In the next section we choose the number of assimilation to be 12 times.

3.2: Experiment 2: with terrain

In this experiment a north-south oriented mountain with the peak height 3,000 m is placed near the center of the domain. It is also assumed that before the mountain, the radar data are available from the surface. But behind the mountain, the observational data are only available above 3,000 m. The purpose of this design is to imitate the scenario of terrain blockages of the radar data. A prevailing westerly wind of 10 ms^{-1} is superimposed to the domain, so that the storm is moving toward the east. Figure 4 denotes the model-predicted wind field and reflectivity at Z=2.5 km after 12 radar data assimilations for experiment 2. The assimilation window

ends at T=80 min. Figure 5 plots the accumulated rainfall over every 5 min. A close examination indicates that with sufficient number of assimilations, the main body of the storm has been accurately recovered before it reaches the mountain. The result at T=60 min reveals that below 3,000 m and behind the mountain, where the radar beams are completely blocked by the terrain, the pattern of the storm still resembles its true counterpart. The successful recovery of the storm before the mountain enables the storm to evolve consistently with the true solution even after passing the mountain. The spatial correlation and the Gilbert Skill Score of the QPF are displayed in Fig 6. It can also be seen that after the last data assimilation at T=80 min, rainfall prediction remains reliable for approximately another 90 min.

4. Summary:

In this study the EnSRF is applied to investigate its performance in terms of improving the QPF for a cloud scale convective system. It is found that in order to make one-hour forecast of the rainfall, at least one hour of data assimilation, or 12 sets of radar data, are also required. The terrain blockage does not seem to impose serous problems to the forecasts, as long as the storm has been recovered reasonably well before it hits the mountain.

Reference:

Evensen, G., 1994: Sequential data assimilation with a nonlinear quasi-geostrophic model using Monte Carlo methods to forecast error statistics, *J. Geophys. Res*., **99** (C5), 10143-10162.

Ming, X., M., Tong, and K. Droegemeier, 2006: An OSSE framework based on the Ensemble square root Kalman filter for evaluating the impact of data from radar networks on thunderstorm analysis and forecast, *J. Atmos. Oceanic Technol.*, **23**, 46-65.

Schaefer, J. T., 1990: The critical success index as an indicator of warning skill, *Wea. and Forecasting*, **5**, 570-575.

Snyder, C., and F. Zhang, 2003: Assimilation of simulated Doppler radar observations with an ensemble Kalman filter, *Mon. Wea. Rev.*, **131**, 1663-1677.

Tong, M., and M. Xue, 2005: Ensemble Kalman filter assimilation of Doppler radar data with a compressible nonhydrostatic model: OSS experiments, *Mon. Wea. Rev*., **133**, 1789-1807.

Whitaker, J. S., and T. M. Hamill, 2002: Ensemble data assimilation without perturbed observations, *Mon. Wea. Rev*., **130**, 1913-1924.

Xue, M., K. K. Droegemeier, V. Wong, 2000: The Advanced Regional Prediction System (ARPS) - A multiscale nonhydrostatic atmospheric simulation and prediction tool, Part I: Model dynamics and verification, *Meteor. Atmos. Phys*., **75**, 161-193.

____, and Coauthors, 2001: The Advanced Regional Prediction System (ARPS)- A multiscale nonhydrostatic atmospheric simulation and prediction tool, Part II: Model physics and applications, *Meteor. Atmos. Phys*., **76**, 143-165.

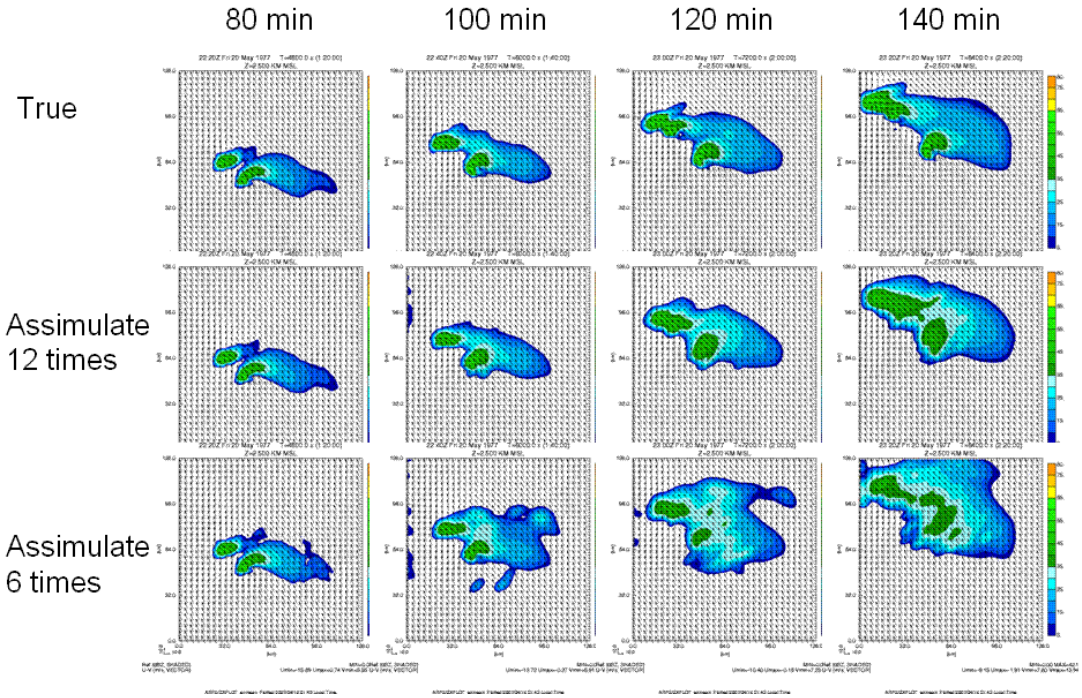

Fig. 1 The reflectivity and wind field at Z=2.5 km at 80, 100, 120 and 140 min for experiment 1. Note that the assimilation window ends at 80 min. The upper panel is the true solution, while the forecasts after 12 (test 1) and 6 (test 2) assimilations are shown in the middle and lower panels, respectively.

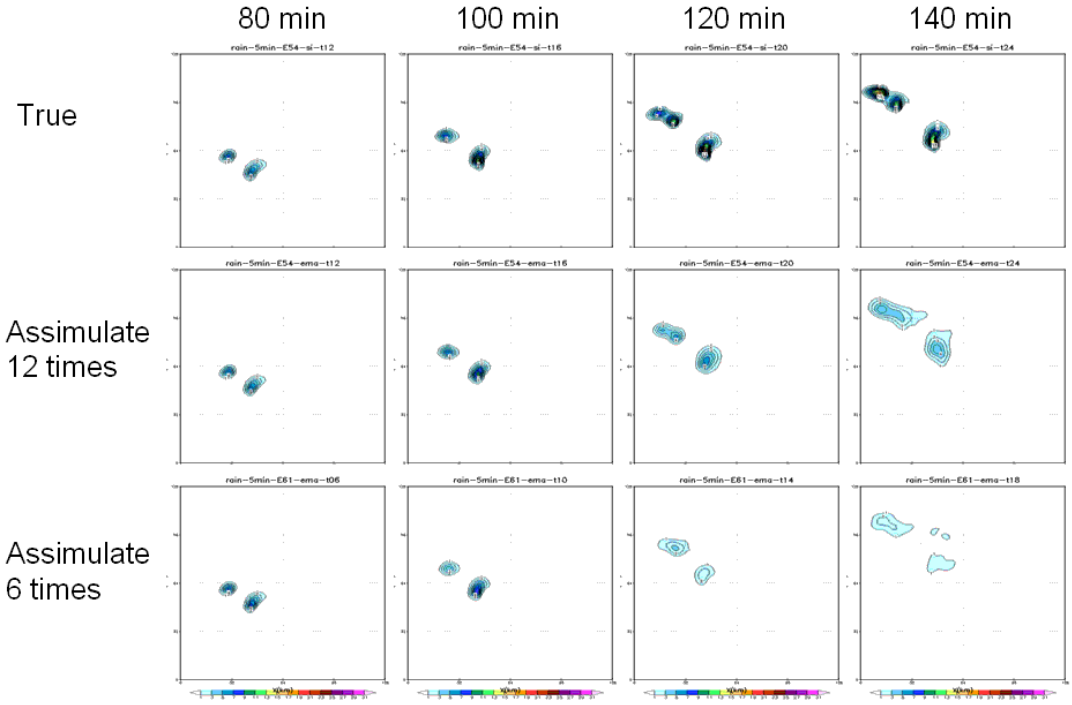

Figure 2 Same as Figure 1, but is the accumulated rainfall over every 5 min.

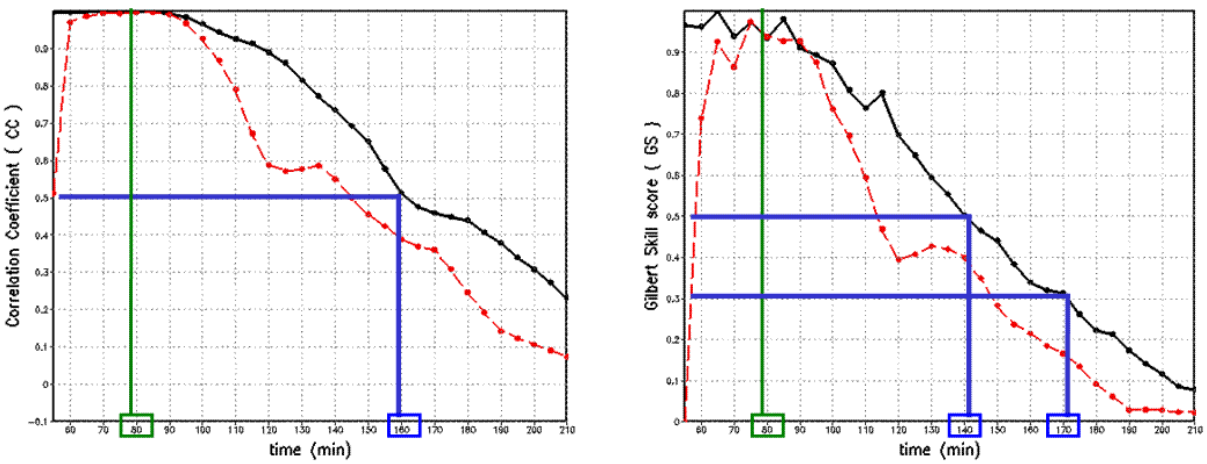

Figure 3 The spatial correlation of the 5 min accumulated rainfall (left panel), and Gilbert Skill Score (right panel). The solid/black and dashed/red lines are for the test 1 (12 assimilation) and test 2 (6 assimilation), respectively. The assimilation ends at T=80 min.

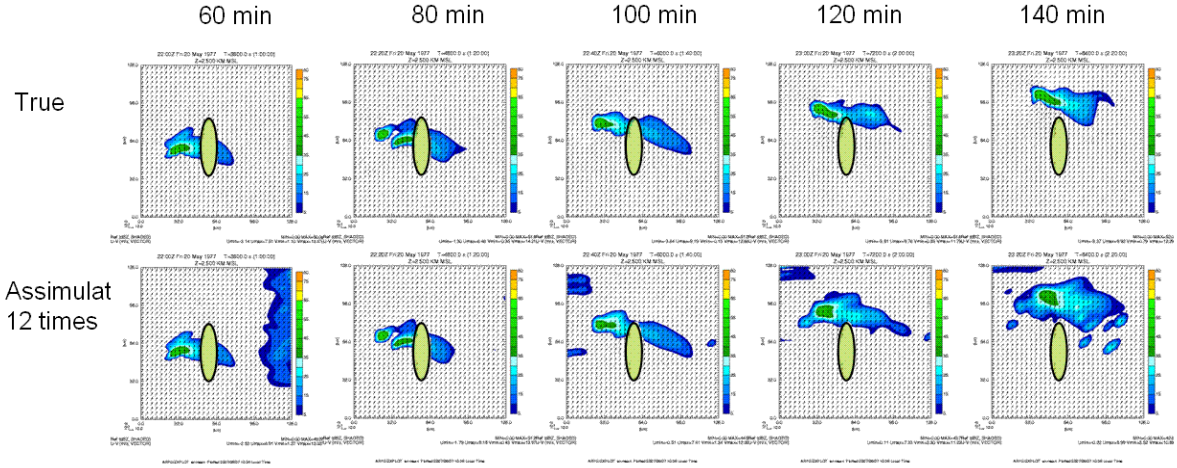

Figure 4 The model-predicted wind field and reflectivity at Z=2.5 km after 12 radar data assimilations for experiment 2. The assimilation window ends at 80 min. The north-south oriented mountain is placed at the center of the domain.

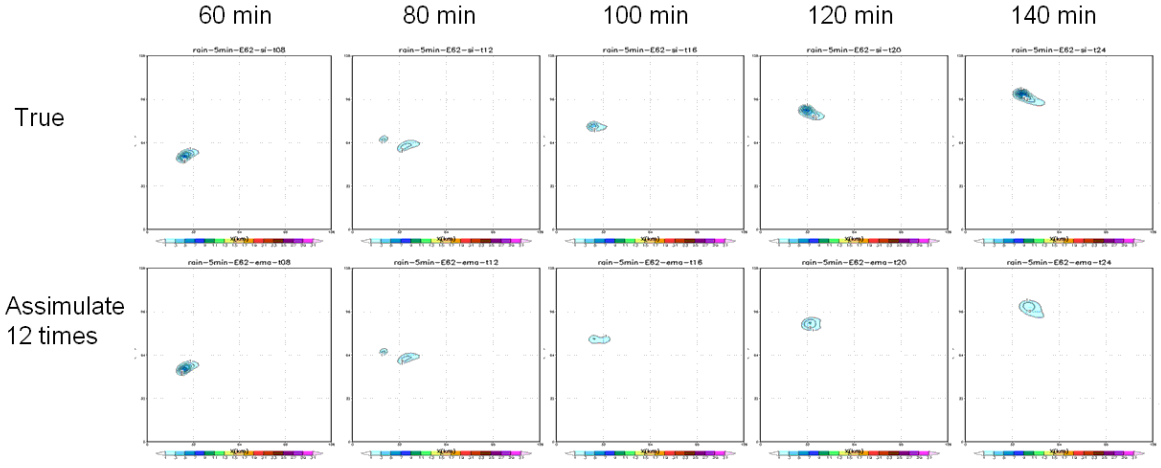

Figure 5 Same as Figure 4, but is the accumulated rainfall over every 5 min.

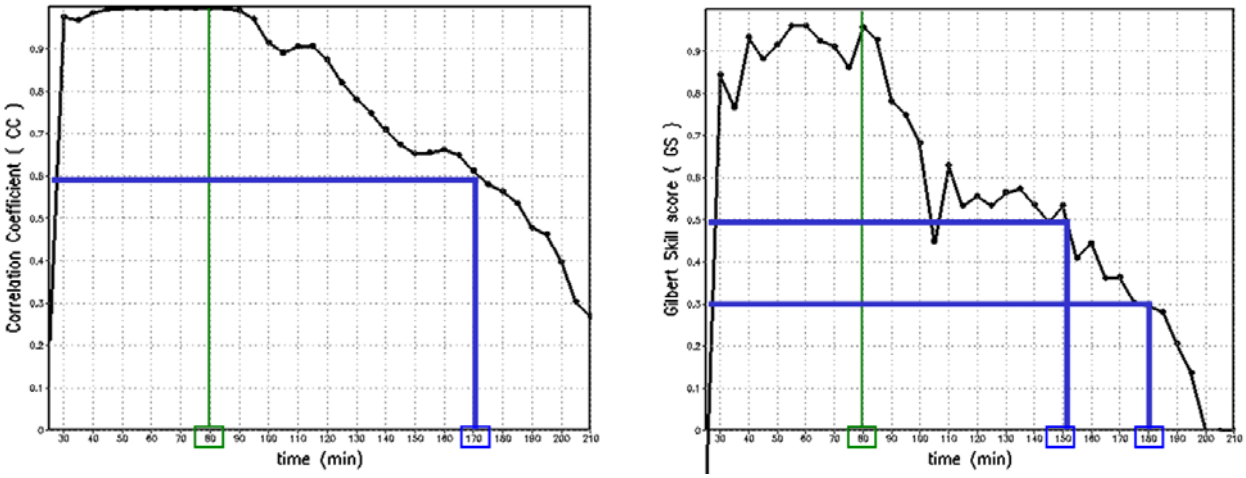

Figure 6 The spatial correlation of the 5 min accumulated rainfall (left panel), and Gilbert Skill Score (right panel), from experiment 2. The assimilation ends at T=80 min.